Geological Mapping of Badondo and Iron Mineralisation Targets, Republic of Congo

MICHAEL CUNNINGHAM[1] and BERT DE WAELE[2]

Introduction

The Badondo – Belinga (North) iron Project (Project) is a greenfields exploration play operated by Equatorial Resources Ltd. (EQX), in dense rainforests of northern Congo (Figure 1). No geological maps existed covering the project, but the French Geological Survey (BRGM) had demonstrated the presence of oxidised BIF with grades of surface samples up to 60% Fe. EQX commissioned an airborne geophysical survey, and SRK was engaged to provide structural mapping over two magnetic targets defined from that data, Badondo and Belinga North (Figure 2).

The study resulted in an improved understanding on the distribution and timing of rock types and structures within the prospect, and identified controls on iron mineralisation. The geological map and insights into the evolution of the region formed the basis of a scout drilling program at the prospect which is currently underway.

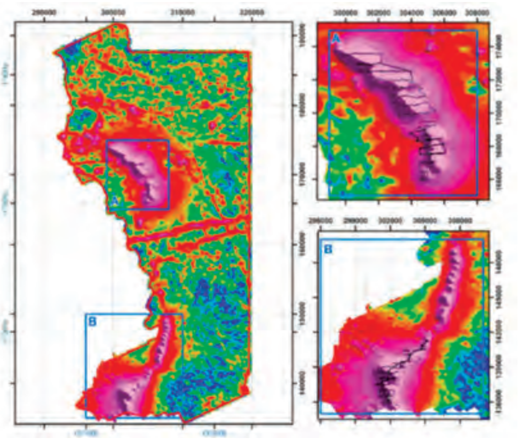

Figure 2 : Analytical signal magnetic data and GPS track logs over the Badondo (A) and Belinga North (B) anomalies

Regional Setting

The Project is located in the northwestern part of the Archaean Congo Craton, within the Chaillu Block, which is comprised of a metamorphosed complex of Tonalite-Trondhjemite-Granite gneisses in which linear belts of metavolcaniclastic rocks and BIF occur. This Archaean assemblage is unconformably overlain by a metasedimentary succession of conglomerate and sandstone including minor volcanic units and chert layers known as the Francevillian Group, and presumed to be Palaeoproterozoic in age.

Figure 1: Location map of Badondo and Belinga, Republic of Congo.

Results of the Geological Mapping

The area is covered by dense primary rain forest, resulting in mapping being conducted along cut lines across the geophysical targets, spaced 400 meters apart. Each mapping team worked on ruggedized PDA's, using a customised set of data capturing tools in ArcPAD™ to record point observations and record contacts and structural data. The dense forest canopy made the use of satellite imagery and aerial photographs impractical, and therefore Digital Terrain and airborne magnetic data (Analytical Signal, Reduced To Equator) were used as base maps. Outcrop at Badondo was ubiquitous and abundant and this paper therefore focuses on the Badondo target area.

Lithology

The work confirmed that Badondo Hill is almost entirely composed of BIF for a distance of about 10 km, with minor occurrence of schist (Figure 5). Based on sericite-

1. SRK Consulting (Australasia), Melbourne (mcunningham@srk.com.au)
2. SRK Consulting (Australasia), West Perth (bdewaele@srk.com.au)

Figure 3 : F2 folds in the BIFs at Badondo

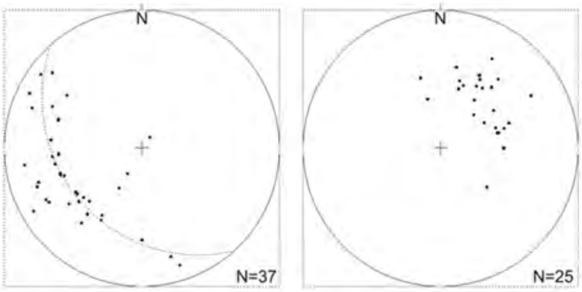

Figure 4 : Equal area stereoplot for S1 and S2 foliations (left) and L2/1 lineations at Badondo Hill

muscovite-plagioclase assemblages in the schist and slight recrystallization of the BIF the grade of metamorphism is assumed to be in the greenschist or lower-amphibolite facies. The country rock is comprised of very poorly exposed granitic gneisses, which were found exposed only in a few locations at the base of the ridge. Based on exposed in situ outcrops, the width of the BIF in plan view is between 200 and 600 m. The BIF is variably oxidised, and can be subdivided into a less-oxidised magnetite BIF, occupying the western part of Badondo Hill and Belinga North, and a more hematititic BIF unit in the eastern half of Badondo. Locally, outcrops of strongly hematitised BIF and massive hematite occur, often in areas of closely spaced jointing that also coincide with breaks in the analytical magnetic signal (demagnetised zones).

Abundant lateritised scree deposits occur on the slopes of Badondo Hill, mainly along the eastern flank, which contain angular fragments of BIF, cemented by goethite and hematite.

Structure

SRK recognised three deformation events in the prospect. Despite multiple phases of deformation, remnant bedding (S_0) in the BIF is preserved in alternating quartz-magnetite layering. F_1 folds are tight to isoclinal cm- to m-sized folds, and are accompanied by steep east-dipping axial-planar S_1 foliations. Steep, prominent lineations are recorded on the S_1 surfaces, which are subparallel to hinges of steeply plunging tight to isoclinal F_2 folds (Figure 3). $L_{2/1}$ lineations plunge around 50° towards 040°, parallel to a β-axis calculated from the S_1 foliations (Figure 4).

A later, regional open folding event (D_3), with steeply plunging or sub-vertical fold hinges is interpreted from the large-scale rotation of the S_1/S_2 foliation along the crest of the Badondo Ridge. However, no penetrative fabrics were observed in the field that could be ascribed to this F_3 folding event. All along the Badondo ridge, an ENE-striking fracture set can be inferred from the magnetic data, possibly related to D_3 deformation, or perhaps reflecting post D_3 brittle deformation.

Mineralisation

Iron mineralisation at Badondo Hill is in form of oxidised BIF comprised of hematite, magnetite and quartz. Surface grades are variable, up to 70.2% Fe, with grade directly correlated with hematite content. The distribution of the iron mineralisation shows a clear pattern with overall lower grades along the western flank of the hill, and higher grades in the east. This corresponds in the field with the presence of less altered magnetite and magnetite-hematite BIF in the west and an increasing prevalence of hematitised BIF in the east. Locally, extremely oxidised BIF units occur, coincident with areas of reduced magnetic signal and closely-spaced jointing. Extensive lateritised scree deposits occur all across the hill, but appear to be more extensive along the steep eastern flank. Based on outcrop, these cemented scree deposits can extend up to 500 meters away from the foot of Badondo Hill.

Genetic Models

The close correlation between the presence of hematitised BIF with fracture sets, and demagnetised zones suggest that enhanced permeability related to more intense fracturing and jointing, and hence oxidation of magnetite to hematite, forms a main driver for mineralisation at Badondo Hill. One zone of intense hematitisation in the southern half of the hill also coincides with the hinge of the large-scale F_3 fold, perhaps reflecting an increased permeability along the F_3 hinge.

The present distribution of iron mineralisation at Badondo Hill, with higher grade units structurally above lower grade BIF, is interpreted to suggest that the BIF acted as an aquitard with respect to drainage along the eastern slope of the hill, resulting in increased oxidation.

Conclusions

Structural mapping has provided, for the first time, an understanding of BIF composition and the delineation of strongly oxidised and hematite-enriched zones associated with cross-cutting fault and fracture sets at Badondo and Belinga North (Figure 5). The geological map and structural data were integrated into a first-pass LeapFrog™ 3D model (Figure 6) that helped to visualise the distribution of rock units and mineralisation from 2D to 3D space, which then formed the basis for the development of a scout drill plan to test for iron mineralisation.

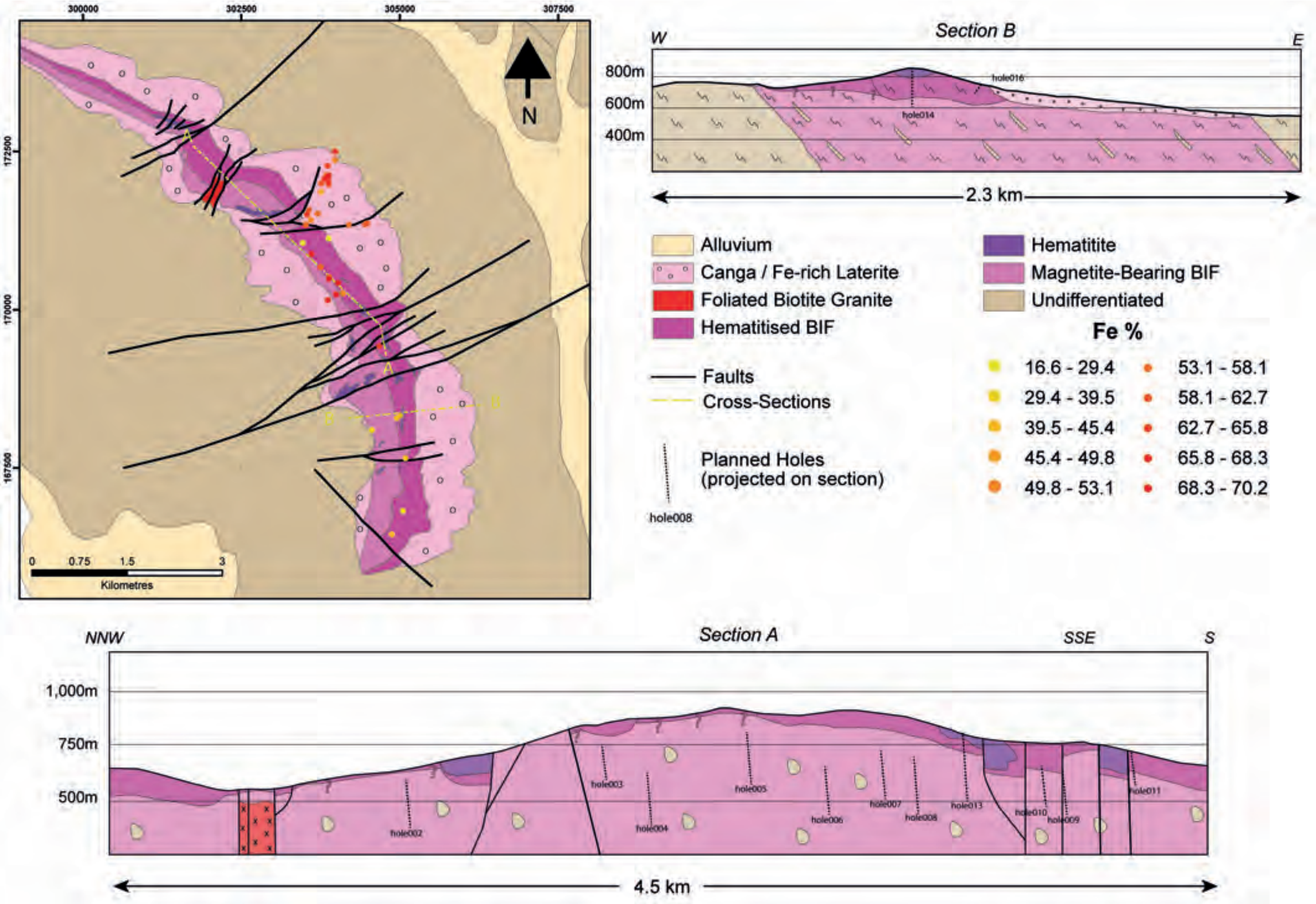

Figure 5 : Interpreted geology and structure of Badondo.

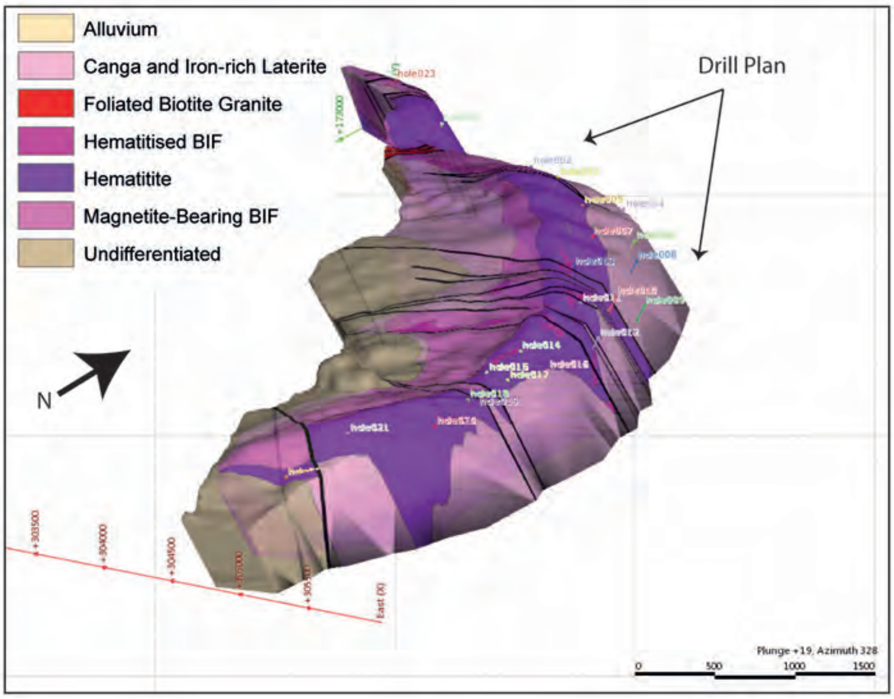

Figure 6 : Badondo 3D geology and structural model of recommended drill targets.